NOTES AND CORRESPONDENCE

The Effect of Changes in Observational Coverage on the Association between Surface Temperature and the Arctic Oscillation

ANTHONY J. BROCCOLI, THOMAS L. DELWORTH, AND NGAR-CHEUNG LAU

NOAA Geophysical Fluid Dynamics Laboratory, Princeton University, Princeton, New Jersey

7 November 2000

ABSTRACT

The effect of changes in observational coverage on the association between the Arctic oscillation (AO) and extratropical Northern Hemisphere surface temperature is examined. A coupled atmosphere–ocean model, which produces a realistic simulation of the circulation and temperature patterns associated with the AO, is used as a surrogate for the real climate system. The association between the AO and spatial mean temperature, as quantified by regressing the latter on the AO index, is subject to a positive bias due to the incomplete spatial coverage of the observational network. The bias is largest during the early part of the twentieth century and decreases, but does not vanish, thereafter.

1. Introduction

Considerable attention has been focused on spatial and temporal variations of temperature during the last several decades in an effort to separate the effects of natural climate variability from those of putative anthropogenic global warming. Motivated by the identification of prominent spatial patterns of atmospheric variability and their associated surface temperature anomalies, a number of studies have attributed a substantial fraction of recent Northern Hemisphere (NH) temperature trends to temporal fluctuations in extratropical circulation.

Of particular interest is the proposed relationship between NH extratropical mean temperature and the Arctic oscillation (AO). The AO, as defined by Thompson and Wallace (1998, 2000), is a pattern of atmospheric variability characterized by a zonally symmetric redistribution of atmospheric mass between the Arctic and midlatitudes, extending from the lower stratosphere to the surface. The AO bears some similarity (Deser 2000) to the North Atlantic oscillation (NAO), which is a more regional measure of the sea level pressure gradient between the Azores high and the Icelandic low (van Loon and Rogers 1978; Barnston and Livezey 1987; Hurrell 1995). Time series of both the AO and NAO have exhibited pronounced positive wintertime trends during the past several decades, a period during which surface temperatures over the NH extratropics have warmed considerably. Thompson et al. (2000) have associated ~30% of the recent wintertime warming of the extratropical NH with the multidecadal trend in the AO. A similar association between spatial mean temperature and the NAO was previously identified by Hurrell (1996).

Studies such as those described above quantify the association between the AO and NAO indices and spatial mean temperature using linear regression and linear correlation. In the sections that follow, a similar approach is adopted. The regression coefficient of extratropical NH temperature on the AO index, $b_{\overline{T},\mathrm{AO}}$, is computed as an estimate of the association between these two quantities. Output from a long integration of a coupled climate model is used to determine to what extent such estimates are affected by variations in observational coverage during the period of instrumental records.

2. Simulation of the AO and its thermal signature

An unforced coupled atmosphere–ocean model simulation is used in this study to explore the effects of temporal variations in spatial sampling on $b_{\overline{T},\mathrm{AO}}$. Both components of the coupled model are three-dimensional, global general circulation models. The atmospheric component represents the horizontal distributions of variables in both spectral and gridpoint domains, with rhomboidal truncation at zonal wavenumber 30 and a

Corresponding author address: Dr. Anthony J. Broccoli, NOAA Geophysical Fluid Dynamics Laboratory, Princeton University, P.O. Box 308, Forrestal Campus, U.S. Route 1, Princeton, NJ 08542.
E-mail: ajb@gfdl.gov

2.25° by 3.75° latitude–longitude grid. The vertical distributions of variables are represented using 14 unevenly spaced finite-difference levels. The oceanic component employs a 2.25° by 1.875° latitude–longitude grid with 18 finite-difference levels. A similar model was used by Knutson et al. (1999) and Delworth and Knutson (2000) to compare observed regional and global temperature trends with those simulated in response to anthropogenic forcing.

As in Thompson and Wallace (1998), the AO index for the coupled model simulation is based on a principal component analysis of monthly sea level pressure (SLP) anomalies over the northern extratropics during the cold season (November–April). To facilitate its comparison with the observations, the AO index time series is linearly scaled such that a value of unity corresponds to a 1-mb SLP difference between the midlatitude and subpolar extrema of its associated spatial pattern.

To assess the realism of the simulated AO, regression coefficients of local SLP on the AO index $b_{\mathrm{SLP,AO}}(x)$ for each grid point x are computed based on 900 years of model output (Fig. 1a) and observations from the period 1899–1997 (Fig. 1b). Observed SLP anomalies are from an extension of the Trenberth and Paolino (1980) dataset obtained through the Web site of the National Center for Atmospheric Research. Both patterns exhibit the annular mode documented by Thompson and Wallace (1998, 2000), with negative SLP values in high latitudes and positive values in midlatitudes. In both the model and observations, negative centers appear near Iceland with positive centers over the North Pacific and from southwestern Europe westward into the North Atlantic. The spatial correlation between the simulated and observed $b_{\mathrm{SLP,AO}}(x)$ patterns over the region north of 20°N is 0.95. Using the standard deviation of the AO index as a measure of the amplitude of AO variability, the coupled model's value of 9.2 mb is quite similar to the observed value of 8.8 mb. The realism of the AO in the coupled model, consistent with analyses of Limpasuvan and Hartmann (1999, 2000) using the atmospheric component of the same model, suggests that useful insights may be gained from further analysis of the simulated AO–temperature relationship.

A similar regression analysis is used to estimate $b_{T,\mathrm{AO}}(x)$, the thermal signature associated with a 1-mb increase in the AO index. To maximize the comparability with the observed data, which are computed from a merged dataset that combines surface air temperature anomalies over land (Jones 1994) and sea surface temperature anomalies elsewhere (Parker et al. 1995), the surface temperatures from the coupled model are a combination of the temperature of the lowest atmospheric model level ($\sim$25 m above the surface) for land points and the uppermost oceanic model level for ocean points. The simulated and observed thermal signatures (Fig. 1) exhibit a pattern correlation of 0.79. The extrema in the temperature patterns have similar placement, with positive $b_{T,\mathrm{AO}}(x)$ values over much of northern Eurasia and

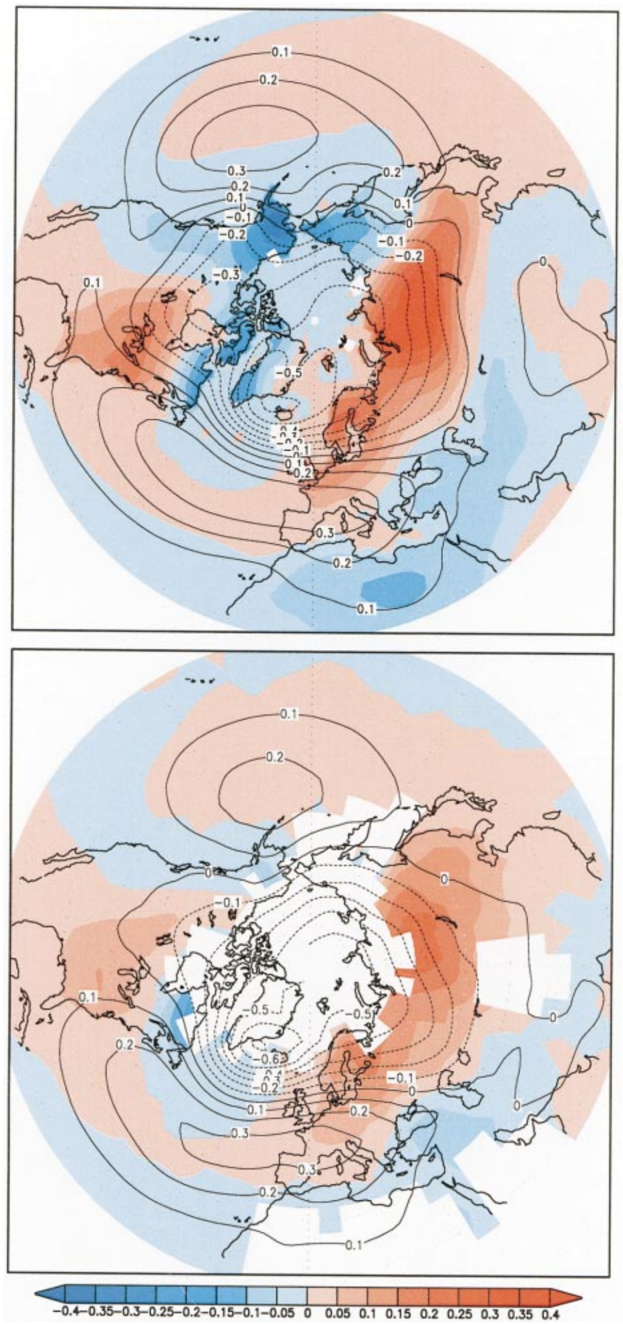

FIG. 1. Regression coefficients of surface temperature [$b_{T,\mathrm{AO}}(x)$, colors, K mb^{-1}] and sea level pressure [$b_{\mathrm{SLP,AO}}(x)$, contours, mb mb^{-1}] on the AO index from (a) the climate model and (b) observations. Model-derived coefficients are based on 900 years of output from an integration with no transient forcing, and observed coefficients are based on data from 1899 to 1997. Unshaded regions in (a) indicate the presence of sea-ice cover; in (b) they indicate that data are available for less than one-half of the months during the 1899–1997 period. Regression coefficients are based on monthly means for the period Nov–Apr.

the eastern United States and negative values over northwestern North America, eastern Canada, and Greenland, and from northern Africa through southwestern Asia. The extreme values of $b_{T,\mathrm{AO}}(x)$ have magnitudes of 0.1–0.4 K mb^{-1}. The fidelity of the coupled model in reproducing the observed AO allows the model to be used to assess the impact of spatial sampling on the relationship between the AO and hemispheric mean temperature.

3. Effect of variations in spatial sampling of surface temperature

To estimate the effects of spatial sampling on $b_{\overline{T},\mathrm{AO}}$, six nonoverlapping 99-yr segments are chosen from the coupled model integration. The duration of these segments is selected to match that of the observed AO index time series. For each of these segments, time series of spatial mean temperature over the NH extratropics are computed in two different ways. In the first computation, all model grid points for the region from 20° to 90°N are averaged (using area weighting), yielding a temperature anomaly time series $\overline{T}^{\mathrm{all}}(t)$. In the second computation, a time-varying ''observational mask'' is determined, which represents the spatial coverage of available data from the observed surface temperature dataset for the period 1899–1997. Surface temperature anomalies from the coupled model are interpolated to this observational mask and spatially averaged to define an additional temperature anomaly time series $\overline{T}^{\mathrm{masked}}(t)$. Because the spatial coverage of the observed surface temperature data is incomplete, $\overline{T}^{\mathrm{all}}(t)$ and $\overline{T}^{\mathrm{masked}}(t)$ generally differ.

To determine how estimates of the AO–temperature relationship are affected by temporal variations in spatial sampling of surface temperature, a ''moving-window'' regression analysis is employed. In this analysis, a time series $b_{\overline{T},\mathrm{AO}}(t)$ is computed by regressing the spatially averaged temperature anomalies for the NH extratropics on the AO index for each of the overlapping 50-yr periods ending on year t. The 50-yr length of the moving window is chosen to be long enough that a relatively large sample is available for the regression analysis, yet short enough to be sensitive to temporal variations in the observational mask. For each of the six coupled model segments, two time series of regression coefficients $b_{\overline{T},\mathrm{AO}}(t)$ are computed, one using $\overline{T}^{\mathrm{all}}(t)$ and the other using $\overline{T}^{\mathrm{masked}}(t)$. A difference time series $\Delta b_{\overline{T},\mathrm{AO}}(t)$ is then computed by subtracting the $b_{\overline{T},\mathrm{AO}}(t)$ values computed using $\overline{T}^{\mathrm{all}}(t)$ from $b_{\overline{T},\mathrm{AO}}(t)$ values computed using $\overline{T}^{\mathrm{masked}}(t)$. The $\Delta b_{\overline{T},\mathrm{AO}}(t)$ values from the six segments are then averaged to form an ensemble mean (Fig. 2, solid line).

The ensemble mean $\Delta b_{\overline{T},\mathrm{AO}}(t)$ time series is positive, indicating that the $b_{\overline{T},\mathrm{AO}}(t)$ values based on the masked coupled model output exhibit a positive bias relative to those computed using complete sampling. The bias decreases in magnitude as the spatial sampling becomes more complete with time, eventually reaching a value of ~0.004 K mb^{-1} in the latter portion of the record.

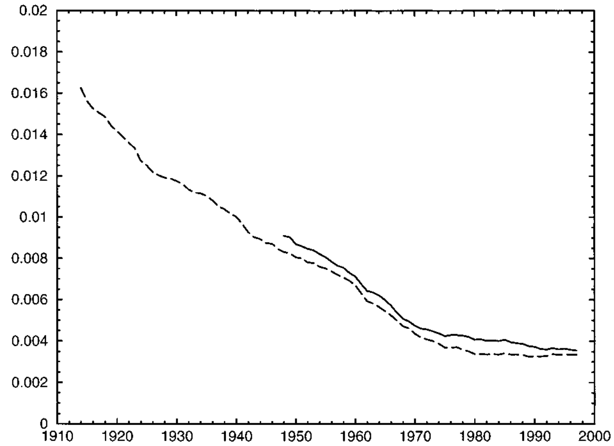

Fig. 2. Model-derived time series of the ensemble mean difference between values of regression coefficients $b_{\overline{T},\mathrm{AO}}(t)$ (solid line) and $b_{\overline{T},\mathrm{NAO}}(t)$ (dashed line) computed using an observational mask that mimics the time-varying spatial sampling in the observed temperature record, and those computed using complete spatial sampling. The ensemble means are based on six nonoverlapping segments of the model integration. Regression coefficients are based on monthly means for the period Nov–Apr.

To understand the reasons for this positive bias, it should be noted that the relationship between NH extratropical mean temperature and the AO index can be regarded as the relatively weak residual that remains after the near cancellation of much larger positive and negative regional temperature anomalies (see Fig. 1). Thus comparable sampling of the positive and negative anomaly regions is necessary to accurately estimate $b_{\overline{T},\mathrm{AO}}$. The positive bias arises because the positive anomaly centers over eastern North America and northern Eurasia are well sampled even in the early twentieth century, since many of the longest observed temperature records are located in these regions. In contrast, the centers of negative correlation tend to be poorly sampled in the early years of the observational record, but become better sampled over time. The relatively poor sampling of surface temperatures over high-latitude North America (see unshaded areas in Fig. 1b) is largely responsible for the positive bias of ~0.004 K mb^{-1} that remains even in recent decades.

The same methodology is used to estimate the effects of spatial sampling on the association between extratropical NH temperature and the NAO index, as expressed by the regression coefficient of the former on the latter, $b_{\overline{T},\mathrm{NAO}}$. The NAO index represents the anomalous SLP difference between the model grid points nearest Ponta Delgada, Azores, and Reykjavik, Iceland, following the definition of the NAO discussed in Jones et al. (1997). In this case, the coupled model segments used are 133-yr long to match the length of the observed NAO time series (Fig. 2, dashed line). The bias in

$b_{\overline{T},\mathrm{NAO}}(t)$ is very similar to that of $b_{\overline{T},\mathrm{AO}}(t)$ during the period of overlap between the two time series. The similarity arises from the strong resemblance of the thermal signature of the NAO (not shown) to that of the AO. The largest bias in $b_{\overline{T},\mathrm{NAO}}(t)$ is associated with moving windows based on the earliest part of the instrumental climate record, a period when there were very few observations from northern North America, northern Africa, and central Asia, all of which are regions where temperature anomalies are negatively correlated with the NAO index. Osborn et al. (1999) speculated that the relatively large correlations between the NAO index and December–February extratropical NH temperature in the early portion of their moving window analysis may be the result of biased spatial sampling. The existence of a large positive bias in $b_{\overline{T},\mathrm{NAO}}(t)$ during the late nineteenth century (Fig. 2, moving windows ending prior to 1950) supports their conjecture.

4. Implications for recent temperature trends

The results of the previous section suggest that regression estimates of the association between the AO and extratropical NH temperature are subject to a positive bias, particularly for periods in the early twentieth century. The bias is smallest for 50-yr moving windows ending after 1970 (Fig. 2), indicating that the least biased estimates of $b_{\overline{T},\mathrm{AO}}$ can be obtained using data for the period from 1920 through the present. In keeping with this approach, $b_{\overline{T},\mathrm{AO}}$ is computed using monthly data from the January–February–March (JFM) season, the so-called ''active season'' of Thompson and Wallace (2000), from the period 1920–97. This procedure yields a $b_{\overline{T},\mathrm{AO}}$ value of 0.019 K mb^{-1}.

As noted by Thompson et al. (2000), there has been a pronounced upward trend in the AO index during the last three decades. The linear trend in this index for the JFM season for the period 1968–97, computed as the slope of a straight line fitted using least squares, is 16.2 mb (30 yr)$^{-1}$. Over the same period, $\overline{T}_{20-90\mathrm{N}}$ during JFM warms by 1.02 K (30 yr)$^{-1}$. The portion of this warming associated with the AO trend can be estimated by multiplying the AO trend by $b_{\overline{T},\mathrm{AO}}$. Based on this procedure, a trend of 0.019 K mb^{-1} $\times$ 16.2 mb (30 yr)$^{-1}$, or 0.31 K (30 yr)$^{-1}$, is associated with the AO trend. This corresponds to ~30% of the overall temperature trend during this period and is consistent with the results of Thompson et al. (2000). (One should note that the fraction of the 30-yr warming trend associated with the AO decreases to ~8% if the spatial domain is extended to the entire Northern Hemisphere and annually averaged temperatures are considered.) The half-width of the 90% confidence interval for the regression coefficient of $\overline{T}_{20-90\mathrm{N}}$ on the AO index (assuming one degree of freedom per year) is 0.005 K mb^{-1}, or ~25% of the value of the coefficient itself. A comparable degree of uncertainty also should be applied to estimates of the temperature trend associated with the recent AO trend.

The lingering positive bias in $b_{\overline{T},\mathrm{AO}}$ after 1970 (Fig. 2), which results from incomplete spatial sampling, implies that the calculation in the previous paragraph overestimates the portion of the recent trend in $\overline{T}_{20-90\mathrm{N}}$ associated with the AO trend. If the spatial sampling bias in $b_{\overline{T},\mathrm{AO}}$ in the real climate system is the same as model-derived estimate, an adjustment for the bias can be made by subtracting the time-dependent values of $\Delta b_{\overline{T},\mathrm{AO}}(t)$ (Fig. 2) from $b_{\overline{T},\mathrm{AO}}$ values based on observations. For the $b_{\overline{T},\mathrm{AO}}$ value computed from observations for the period 1920–97, an adjustment of ~0.004 K mb^{-1} is used, which is a typical value of $\Delta b_{\overline{T},\mathrm{AO}}(t)$ for moving windows ending from 1970 to the present. Applying this model-derived adjustment yields an adjusted $b_{\overline{T},\mathrm{AO}}$ value of 0.015 K mb^{-1}, so the portion of 1968–97 trend in $\overline{T}_{20-90\mathrm{N}}$ during JFM associated with the AO is reduced from 0.31 K (30 yr)$^{-1}$ to 0.24 K (30 yr)$^{-1}$.

To estimate what fraction of the overall trend this 0.24 K (30 yr)$^{-1}$ AO component represents, an adjustment to the incompletely sampled overall trend should also be made. Such an adjustment should account for the sampling biases associated with both the AO component of the overall trend (estimated in the previous paragraph) and the portion of the trend *not* associated with the AO. Unfortunately, an unambiguous estimate of this latter bias is unavailable. In the absence of such information, an assumption can be made that the sampling bias for the ''non-AO'' component of the trend is close to zero. There is some support for this assumption, such as the finding by Madden and Meehl (1993) that the sensitivity of the simulated global warming signal to incomplete spatial sampling is typically less than 2%, although the applicability of this finding is limited by differences in the spatial domain (i.e., global vs NH extratropics). Making the assumption of zero sampling bias for the non-AO component of the trend, the overall trend would be adjusted downward by the same amount as the component associated with the AO, or 0.004 K mb^{-1} $\times$ 16.2 mb (30 yr)$^{-1}$ = 0.07 K (30 yr)$^{-1}$. This estimate of the bias in the extratropical Northern Hemisphere mean temperature trend agrees quite closely with the results of Karl et al. (1994) for trends beginning in the 1970s (their experiment 10MSU), although the spatial and temporal domains are not exactly the same. This adjustment reduces the overall trend from 1.02 K (30 yr)$^{-1}$ to 0.95 K (30 yr)$^{-1}$. Thus the 0.24 K (30 yr)$^{-1}$ adjusted AO component would represent ~25% of the adjusted overall trend.

5. Summary and conclusions

In this study, output from a coupled model integration is used to determine to what extent regression-based estimates of the AO–temperature relationship are affected by variations in observational coverage during the period of instrumental records, yielding the following results.

- The coupled atmosphere–ocean model realistically simulates the spatial patterns of SLP and surface temperature changes associated with variations in the AO index. The correlations between the simulated and observed patterns of SLP and surface temperature are 0.95 and 0.79, respectively.
- When surface temperatures from the coupled model are masked to mimic the availability of instrumental temperature records, imperfect observational coverage leads to an overestimation of the strength of the association between the AO and spatial mean temperature. The magnitude of this spatial sampling bias gradually decreases during the twentieth century, although it does not vanish even during the periods of greatest spatial coverage.
- This spatial sampling bias leads to an overestimation of the portion of the recent wintertime (JFM) extratropical NH warming trend associated with the AO.

These findings highlight the importance of adequate sampling of regional temperature anomalies in determining the association between the AO and extratropical NH mean temperature. This contrasts with the less important impact of spatial sampling on the trend in hemispheric and global mean temperature during the past 100 years, as determined from ''frozen-grid'' diagnostics using observed surface temperature data (Jones et al. 1986a,b). Because the warming during the last century is relatively amorphous in space, it can be more precisely estimated, even from a relatively limited subset of grid points with nonuniform coverage. Using output from a transient climate change simulation as a perfectly sampled surrogate for the real climate system, Karl et al. (1994) have shown that spatial sampling biases associated with centennial temperature trends are an order of magnitude smaller than the trends themselves. This contrasts with the relatively large sampling bias for $b_{\overline{T},\mathrm{AO}}$, which is as much as 50% of the $b_{\overline{T},\mathrm{AO}}$ value during the early part of the AO record. The more distinct spatial structure of the thermal signature of the AO requires more complete sampling or optimum interpolation techniques.

Acknowledgments. The authors thank I. Held, P. Kushner, J. Lanzante, and D. Thompson, for their comments on earlier versions of this paper and the anonymous reviewers for their constructive criticisms during the paper's final preparation. Thanks also to J. Hack for his advice in identifying the proper forum for this work.

REFERENCES

Barnston, A. G., and R. E. Livezey, 1987: Classification, seasonality, and persistence of low-frequency atmospheric circulation patterns. *Mon. Wea. Rev.,* **115,** 1083–1126.
Delworth, T. L., and T. R. Knutson, 2000: Simulation of early 20th century global warming. *Science,* **287,** 2246–2250.
Deser, C., 2000: On the teleconnectivity of the ''Arctic oscillation.'' *Geophys. Res. Lett.,* **27,** 779–782.
Hurrell, J. W., 1995: Decadal trends in the North Atlantic oscillation: Regional temperatures and precipitation. *Science,* **269,** 676–679.
——, 1996: Influence of variations in extratropical wintertime teleconnections on Northern Hemisphere temperature. *Geophys. Res. Lett.,* **23,** 665–668.
Jones, P. D., 1994: Hemispheric surface air temperature variations: A reanalysis and an update to 1993. *J. Climate,* **7,** 1794–1802.
——, S. C. B. Raper, R. S. Bradley, H. F. Diaz, P. M. Kelly, and T. M. L. Wigley, 1986a: Northern Hemisphere surface air temperature variations: 1851–1984. *J. Climate Appl. Meteor.,* **25,** 161–179.
——, ——, and T. M. L. Wigley, 1986b: Southern Hemisphere surface air temperature variations: 1851–1984. *J. Climate Appl. Meteor.,* **25,** 1213–1230.
——, T. Jonsson, and D. Wheeler, 1997: Extension to the North Atlantic oscillation using early instrumental pressure observations from Gibraltar and South-West Iceland. *Int. J. Climatol.,* **17,** 1433–1450.
Karl, T. R., R. W. Knight, and J. R. Christy, 1994: Global and hemispheric temperature trends: Uncertainties related to inadequate spatial sampling. *J. Climate,* **7,** 1144–1163.
Knutson, T. R., T. L. Delworth, K. W. Dixon, and R. J. Stouffer, 1999: Model assessment of regional surface temperature trends (1949–97). *J. Geophys. Res.,* **104,** 30 981–30 996.
Limpasuvan, V., and D. L. Hartmann, 1999: Eddies and the annular modes of climate variability. *Geophys. Res. Lett.,* **26,** 3133–3136.
——, and ——, 2000: Wave-maintained annular modes of climate variability. *J. Climate,* **13,** 4414–4429.
Madden, R. A., and G. A. Meehl, 1993: Bias in the global mean temperature estimated from sampling a greenhouse warming pattern with the current surface observing network. *J. Climate,* **6,** 2486–2489.
Osborn, T. J., K. R. Briffa, S. F. B. Tett, P. D. Jones, and R. M. Trigo, 1999: Evaluation of the North Atlantic oscillation as simulated by a coupled climate model. *Climate Dyn.,* **15,** 685–702.
Parker, D. E., C. K. Folland, and M. Jackson, 1995: Marine surface temperature: Observed variations and data requirements. *Climatic Change,* **31,** 559–600.
Thompson, D. W. J., and J. M. Wallace, 1998: The Arctic oscillation signature in the wintertime geopotential height and temperature fields. *Geophys. Res. Lett.,* **25,** 1297–1300.
——, and ——, 2000: Annular modes in the extratropical circulation. Part I: Month-to-month variability. *J. Climate,* **13,** 1000–1016.
——, ——, and G. C. Hegerl, 2000: Annular modes in the extratropical circulation. Part II: Trends. *J. Climate,* **13,** 1018–1036.
Trenberth, K. E., and D. A. Paolino Jr., 1980: Northern Hemisphere sea level pressure data set: Trends, errors and discontinuities. *Mon. Wea. Rev.,* **108,** 855–872.
van Loon, H., and J. C. Rogers, 1978: Seesaw in winter temperatures between Greenland and northern Europe. Part I: General description. *Mon. Wea. Rev.,* **106,** 296–310.